16. Metal Complexes with Macrocyclic Ligands

Part XXVII[1])

Cu^{2+}-Promoted Hydrolysis of Carboxylic- and Phosphonic-Acid Esters in the Side Chain of Tetraazamacrocycles

by **Daniel Tschudin, Andreas Riesen**, and **Thomas A. Kaden***

Institut für Anorganische Chemie, Spitalstrasse 51, CH-4056 Basel

(10. XI. 88)

The X-ray structures of the Cu^{2+} complexes of 1,4,8,11-tetraazacyclotetradecane derivatives with an ethylpropionate and diethylphosphonate group, **5** and **6**, respectively, indicate that the metal ion is pentacoordinated by the four N-atoms of the macrocycle and one O-atom. In the case of **5**, it is the carbonyl O-atom of the carboxylate group, whereas for **6** it is the phosphonyl O-atom of the phosphonate group. The hydrolysis kinetics of the functional group in the Cu^{2+} complexes with the 1,4,8,11-tetraazacyclotetradecanes **3**–**6** have been measured by pH-stat and stopped-flow techniques. The rate law for the hydrolysis of the carboxylates **3**–**5** is proportional to the complex concentration and to $[OH^-]$ up to pH 13, whereas that of the phosphonate **6** is proportional to $[OH^-]$ up to pH 11.5, becoming independent of $[OH^-]$ at pH > 11.5. The mechanisms of these two reactions are discussed, considering the possibility of an intra- or an intermolecular OH^- attack and the results of the X-ray structure analyses.

Introduction. – In many metalloenzymes, the metal ion at the active site plays a central role in the hydrolysis of esters, amides, and peptides [2] and is essential for enzymatic activity. There are many low-molecular-weight compounds in which metal-induced hydrolysis reactions have been observed and proposed as models for analogous enzymatic process [3]. After the initial work by *Kroll* [4], the hydrolysis of amino-acid esters induced by metal ions has become one of the most throughly investigated reactions of this type. In the discussion of the hydrolytic mechanism, the study of Co^{3+} complexes has also played an important role, because of their chemical inertness and, thus, the possibility to distinguish between different mechanisms [5]. Two main reaction paths were observed: *a*) attack of free OH^- onto the coordinated ester group which is activated through coordination to the metal ion, or *b*) an intramolecular nucleophilic attack of coordinated OH^- onto the ester group. However, in the case of labile metal ions, a clear distinction between these two mechanisms is much more difficult and often impossible.

Having previously observed, that in the Cu^{2+} complex of **2** the rate of nitrile hydrolysis is extremely fast, because of an internal nucleophilic attack of coordinated OH^- [6], we have now prepared the macrocycles **3**–**7**, to investigate, whether other groups at the end of the side chain also undergo enhanced hydrolysis [7]. In one case, the length of the side chain was varied to investigate, whether structural changes of this type would influence

[1]) Part XXVI: [1].

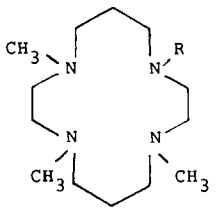

1 R = CH_3
2 R = CH_2–CN
3 R = CH_2–$COOCH_3$
4 R = CH_2–$COOC_2H_5$
5 R = CH_2–CH_2–$COOC_2H_5$
6 R = CH_2CH_2–$PO(OCH_2CH_3)_2$
7 R = CH_2–$CON(CH_3)_2$

the reactivity. In addition, the X-ray structures of the Cu^{2+} complexes of **5** and **6** were determined.

Experimental. – The Cu^{2+} complexes used in this study were prepared as described in [1]. Crystals for X-ray structure analysis were obtained by preparing a sat. soln. of the complex at r.t. and by letting the solvent slowly evaporate in a desiccator filled with $CaCl_2$. The crystal specifications, the experimental conditions, and the results of the X-ray analysis are collected in *Table 1*.

Unit cell parameters were determined by accurate centering of 25 independent strong reflections by the least-squares method. Four standard reflections monitored every h during data collection showed no significant variation of the intensity. The raw data set was corrected for polarization effects, but no correction for absorbance was applied. The structures were solved by *Patterson* techniques using the program SHELXS-86 [8]. Anisotropic least-squares refinements were carried out on all non-H-atoms of the ligand, the Cu^{2+} cation and the Cl-atoms. The Et groups of the phosphonate moiety were isotropically refined, and all H-atoms are in calculated positions. Scattering factors are from *Cromer et al.* [9] or given in the SHELX-76 program. Fractional coordinates are deposited by the *Cambridge Crystallographic Data Centre*.

Table 1. *Crystal Data and Parameters of the Data Collection for the Cu^{2+} Complexes with* **5** *and* **6**

Formula	$C_{18}H_{38}Cl_2CuN_4O_{10}$ [Cu(**5**)]·$(ClO_4)_2$	$C_{19}H_{43}Cl_2CuN_4O_{11}P \cdot 0.5H_2O$ [Cu(**6**)]·$(ClO_4)_2$
Space group	monoclinic, $P2_1/n$	monoclinic, $C2/c$
a [Å]	9.685(9)	27.450(8)
b [Å]	17.339(6)	16.495(3)
c [Å]	15.437(4)	16.783(3)
α [°]	90	90
β [°]	92.99(4)	125.46(3)
γ [°]	90	90
V [Å^3]	2588.8	6189.9
Z	4	8
Crystal size [mm]	0.3 × 0.2 × 0.2	0.3 × 0.3 × 0.2
Temperature	293	293
Θ_{max} [°]	26	25
Radiation	MoK_α (λ = 0.71069 Å)	MoK_α (λ = 0.71069 Å)
Scan type	$\omega/2\Theta$	$\omega/2\Theta$
Collected intensities	$\pm h,+k,+l$	$\pm h,+k,+l$
μ [cm^{-1}]	10.4	4.68
F(000)	1268	2848
No. of ind. reflections	5741	5635
No. of refl. used in ref.	2551 ($F > 3\sigma(F)$)	2520 ($F > 2\sigma(F)$)
No. of variables	349	336
Observations/parameter	7.3	7.5
Largest shift/esd	0.02	0.04
Largest peak on ΔF[e/Å^3]	1.42	0.76
Final R value	0.101	0.093

The kinetics of the hydrolysis were measured either by pH-stat technique or by spectrophotometric measurements at $I = 0.5$M (KNO_3) and 30°. All calculations were accomplished by the program *SANYO* [10].

pH-Stat Measurements. Using a *Metrohm* pH-stat instrument the rate of OH^- consumption (I) during the ester hydrolysis of the Cu^{2+} complexes with **3**, **4**, and **5** ($5 \cdot 10^{-3}$ M) was monitored by addition of 0.1M NaOH so that the pH remained constant.

$$[Cu(L{-}COOR)]^{2+} + OH^- \rightarrow [Cu(L{-}COO)]^+ + ROH \quad (1)$$

From each kinetics curve (ml OH^- as a function of time), 20 experimental points were selected for the calculation of the pseudo-first-order rate constant k_{obs}. The standard deviations of k_{obs} were less than 5%.

Spectrophotometric Measurements. At high pH, hydrolysis of the Cu^{2+} complexes with **3**, **4**, and **5** were followed on a *Durrum* stopped-flow instrument *D110* equipped with a *DATALAB D901* transient recorder on-line with an *Apple II*. The two solns. to be mixed contained $4 \cdot 10^{-4}$ M Cu^{2+} complex in 0.5M KNO_3 and 0.1M 2-(*tert*-butylamino)ethanol of different pH, or NaOH of different concentrations adjusted to $I = 0.5$M, respectively. The reactions were monitored at 550 nm for the complexes with **3** and **4** and at 600 nm for that with **5**. The hydrolysis of the Cu^{2+} complex with **6** ($5 \cdot 10^{-3}$ M) was followed on a *Varian Techtron* spectrophotometer with an automatic cell exchanger at 680 nm and 40° at different pH values using (*tert*-butylamino)ethanol buffer or NaOH. Since the reactions were relatively slow, measurements were done every 30–60 min. For the calculation of the rate constant k_{obs}, 20–30 points were selected. Similarly, the hydrolysis of $[Cu(7)]^{2+}$ was studied, but no spectrophotometric change was observed over a period of 3 days.

Results. – The results of the X-ray structure analysis of $[Cu(\mathbf{5})]^{2+}$ and $[Cu(\mathbf{6})]^{2+}$ are shown in *Figs. 1* and *2*, and selected bond lengths and angles are given in *Table 2*.

In both cases, the Cu^{2+} is pentacoordinate, surrounded by the four N-atoms of the macrocycle and an O-atom of the functional group of the side chain. The geometry can be described either by a distorted square pyramid or a distorted trigonal bipyramid. In the first case, the four N-atoms build the base and the somewhat longer Cu–O bond the apical position of the pyramid. However, the geometry is strongly distorted, since the best plane through the four N-atoms shows deviations of ±0.22 Å and ±0.24 Å for $[Cu(\mathbf{5})]^{2+}$ and $[Cu(\mathbf{6})]^{2+}$, respectively. In addition, the Cu^{2+} is out of this plane by 0.21 Å and 0.30 Å for $[Cu(\mathbf{5})]^{2+}$ and $[Cu(\mathbf{6})]^{2+}$, respectively, in the direction of the apical O-atom. In the second case, we have a nearly linear arrangement for N(1)–Cu–N(3) and two right angles for O(1)–Cu–N(1) and O(1)–Cu–N(3). However, the angles in the equatorial plane differ considerably from the ideal one of 120°. The largest deviations are found for N(2)–Cu–N(4) (155.8° and 149.9°, respectively). The macrocycle is folded along the N(1)–Cu–N(3) axis and assumes the *trans-I (RSRS)* configuration [11] with all substitu-

Table 2. *Selected Bond Lengths* [Å] *and Angles* [°] *for the* Cu^{2+} *Complexes with* **5** *and* **6**

	$[Cu(\mathbf{5})]^{2+}$	$[Cu(\mathbf{6})]^{2+}$
Cu–N(1)	2.084(13)	2.073(11)
Cu–N(2)	2.070(12)	2.080(11)
Cu–N(3)	2.073(12)	2.095(10)
Cu–N(4)	2.069(12)	2.070(12)
Cu–O(1)	2.224(11)	2.161(9)
N(1)–Cu–N(3)	178.9(5)	176.9(5)
N(2)–Cu–N(4)	155.5(5)	149.9(5)
O(1)–Cu–N(1)	90.6(5)	90.4(4)
O(1)–Cu–N(2)	98.8(4)	101.9(4)
O(1)–Cu–N(3)	88.5(4)	92.7(4)
O(1)–Cu–N(4)	105.7(4)	108.2(5)

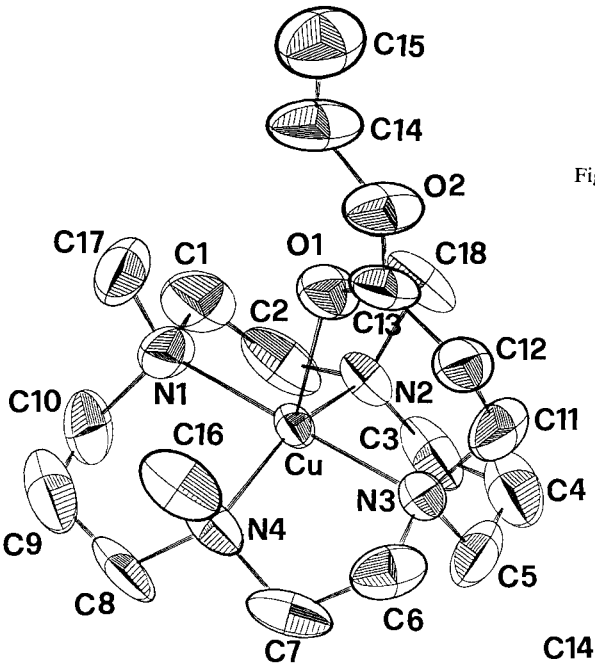

Fig. 1. *ORTEP Plot of the* $[Cu(5)]^{2+}$ *complex*

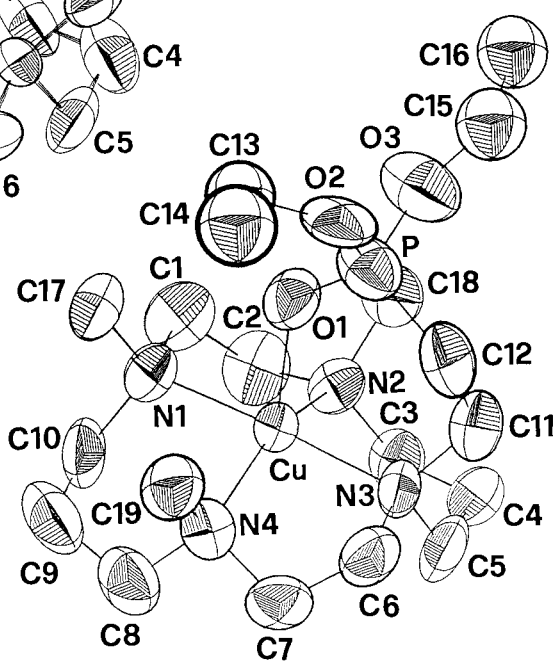

Fig. 2. *ORTEP Plot of the* $[Cu(6)]^{2+}$ *complex*

ents at the N-atoms on the same side of the four N-plane, which is typical for macrocycles with tertiary N-atoms as **1** [12].

Kinetics. The rates of hydrolysis of Cu^{2+} complexes with the carboxylic- and phosphonic-acid esters were measured under pseudo-first-order conditions (pH constant). However, k_{obs} obtained in this way is pH-dependent. *Fig. 3* shows the pH-profile of k_{obs} in the case of the carboxylates **3**–**5**, and it is clear that k_{obs} is proportional to $[OH^-]$ over the whole pH-region studied. Thus the rate law is given by *Eqn. 2*, and the bimolecular rate constants k_{OH}, obtained by fitting the straight lines, are collected in *Table 3*.

$$v = k_{obs} \cdot c_{complex} = k_{OH} \cdot [[Cu(L{-}COOR)]^{2+}] \cdot [OH^-] \qquad (2)$$

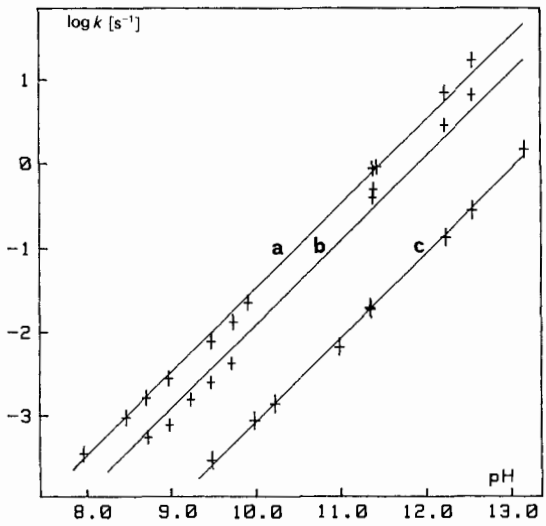

Fig. 3. *pH Profile of* k_{obs} *for the hydrolysis of the ester function in the complex* $[Cu(\mathbf{3})]^{2+}$ (a), $[Cu(\mathbf{4})]^{2+}$ (b), *and* $[Cu(\mathbf{5})]^{2+}$ (c) *at 30°*

Table 3. *Bimolecular Rate Constants for the Alkaline Hydrolysis of Ester Groups in Different Metal Complexes and Amino Acids*

	k [$M^{-1} \cdot s^{-1}$]	T	Lit.
$[Cu(\mathbf{3})]^{2+}$	231 ± 27	30°	–
$[Cu(\mathbf{4})]^{2+}$	84 ± 20	30°	–
$[Cu(\mathbf{5})]^{2+}$	5.9 ± 0.7	30°	–
$NH_2-CH_2-COOCH_3$	1.3	25°	[13]
$^+NH_3-CH_2-COOCH_3$	2.8	25°	[13]
$NH_2-CH_2-COOEt$	0.64	25°	[14]
$^+NH_3-CH_2-COOEt$	23	25°	[14]
$NH_2-CH_2-CH_2COOEt$	0.068	25°	[15]
$(NH_3)_5Co-NH_2-CH_2COOEt^{3+}$	50	25°	[16]
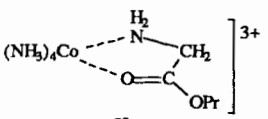	$8 \cdot 10^5$	25°	[17]
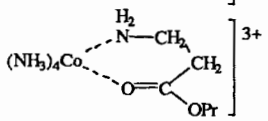	$4 \cdot 10^4$	25°	[17]

In *Fig. 4* the pH dependence of the rate of hydrolysis for $[Cu(\mathbf{6})]^{2+}$ is plotted. At pH < 11.5, the reaction rate is proportional to $[OH^-]$, but at pH > 11.5, a plateau is observed. This pH-profile is, thus, completely different from those of the esters (see above), but resembles that previously observed for the hydrolysis of the Cu^{2+} complex with **2** in which the CN group is hydrolyzed to the amide [6]. The pH dependence can quantitatively be explained by assuming a rapid preequilibrium (*3*), in which a hydroxo complex is formed, followed by the rate-determining step of the hydrolysis (*4*).

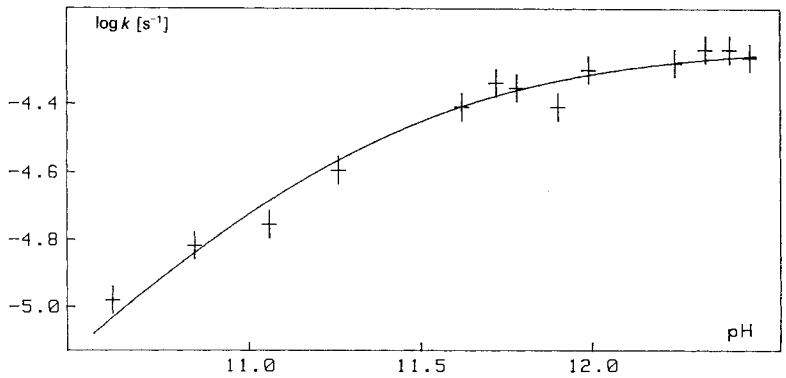

Fig. 4. *pH Profile of* k_{obs} *for the hydrolysis of the phosphonate ester group in* $[Cu(\mathbf{6})]^{2+}$ *at 40°*

$$[Cu(L{-}PO(OEt)_2)]^{2+} + OH^- \overset{K}{\rightleftarrows} [Cu(L{-}PO(OEt)_2)(OH)]^+ \quad (3)$$

$$[Cu(L{-}PO(OEt)_2)(OH)]^+ \overset{k}{\rightarrow} [Cu(L{-}PO_2(OEt))]^+ + EtOH \quad (4)$$

The *Equilibrium 3* is described with an equilibrium constant K *(Eqn. 5)*, whereas k is the limiting rate constant *(Eqn. 6)*.

$$K = [[Cu(L{-}PO(OEt)_2^{2+})]] \cdot [OH^-]/[[Cu(L{-}PO(OEt)_2)(OH)]^+] \quad (5)$$

$$v = k \cdot [[Cu(L{-}PO(OEt)_2)(OH)]^+] \quad (6)$$

Taking into account the stoichiometric *Eqn. 7*, one can calculate the concentration of the hydroxylated species *(Eqn. 8)*.

$$c_{complex} = [[Cu(L{-}PO(OEt)_2)]^{2+}] + [[Cu(L{-}PO(OEt)_2)(OH)]^+] \quad (7)$$

$$[[Cu(L{-}PO(OEt)_2)(OH)]^+] = c_{complex}/(1 + K/[OH^-]) \quad (8)$$

This value introduced in *Eqn. 6* gives the new rate law *(Eqn. 9)*, which can be used to determine K and k by non-linear curve fitting of the experimental data.

$$v = k \cdot c_{complex} \cdot [OH^-]/(K + [OH^-]) = k_{obs} \cdot c_{complex} \quad (9)$$

The values are $K = (2.9 \pm 0.3) \cdot 10^{-3}$ M and $k = (5.9 \pm 0.2) \cdot 10^{-5}$ s^{-1}. The second step of the hydrolysis *(Eqn. 10)* is extremely slow and was not studied kinetically.

$$[Cu(L{-}PO_2(OEt))]^+ + OH^- \rightarrow [Cu(L{-}PO_3)] + EtOH \quad (10)$$

Discussion. – Both structures of the Cu^{2+} complexes with **5** and **6** indicate that the metal ion binds to the functional group of the side chain, so that, in principle, a potential nucleophile could attack the polarized carbonyl or phosphonyl group. It is, however, clear that the general problem concerning structures observed in the solid state and structures present in solution does not allow to transfer the structural results from one

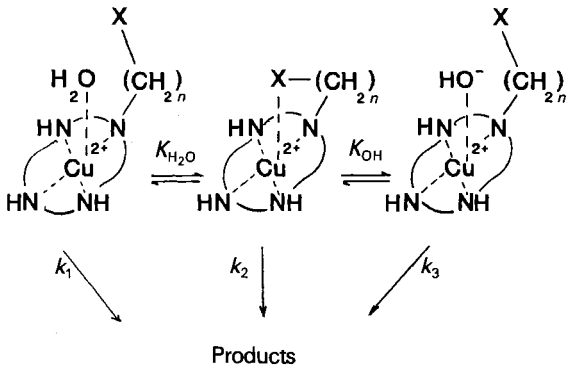

Fig. 5. *Reaction scheme for the hydrolytic cleavage of a functional group in the side chain of a Cu^{2+}-macrocyclic complex*

medium to the other. For a detailed discussion of the hydrolytic cleavage, therefore, the solution behaviour must be known. *Fig. 5* shows the possible species which could be present in alkaline solution. From the complex with a coordinated functional group as observed in the X-ray crystal structure, two new ones can be formed by addition of H_2O or OH^-. Each of these three complexes could be the reactive form for the hydrolysis and has its own reactivity (k_1, k_2, k_3).

In the case of the phosphonate, **6** we find at pH < 11.5 a species with an absorption maximum at 690 nm [1], clearly supporting the coordination of the phosphonate group in the axial position of the Cu^{2+} and, thus, excluding the open form with axial H_2O. At pH > 11.5, there is a rapid colour change to an absorption maximum at 720 nm, indicating a rapid pre-equilibrium to the hydroxylated species. The pH dependence with a plateau at high pH, thus, excludes a bimolecular reaction in the rate-determining step and is a strong indication for an intramolecular nucleophilic attack in the hydroxylated species. In this respect, the hydrolysis of the phosphonate group resembles that of the CN function in **2** which was shown by its pH dependence (similar to the one here) and by competitive inhibition with SCN^- to proceed by an intramolecular mechanism [6].

In the case of the carboxylates **3**–**5**, the absorption spectra in solution indicate that the carbonyl O-atom is also coordinated [1]. However, we do not observe any rapid colour change up to pH ~ 13, which would indicate a hydroxylated species. Since the kinetics remains bimolecular over the whole pH region studied (*cf. Fig. 3*), each of the three possibilities depicted in *Fig. 5* could be the right one: the pathways k_1 and k_2 describing intramolecular reaction between OH^- and the complexes are *per se* bimolecular, and pathway k_3 becomes pseudo bimolecular, if the hydroxylation equilibrium (K_{OH}) is such that only a small amount of the hydroxo species is present.

A comparative study of the rate of ester hydrolysis with a series of Co^{3+} complexes and of amino-acid esters allows to draw some additional conclusions *(Table 3)*. If we compare the rate constants of glycine ethyl ester, the protonated form of glycine ethyl ester, and the monodentate complex $[(NH_3)_5Co(NH_2{-}CH_2COOEt)]^{3+}$, we find an acceleration of a factor of 36 and 78, respectively, based on the glycine ester itself. Thus, a positive charge on the amino N-atom of the ester has a relatively small effect. In our Cu^{2+} complexes, the equilibrium between the open (aquo ion) and closed (coordinated ester)

form is shifted to the side of the closed one (based on the spectra, see above) and only a small amount, probably less than 10%, of the open form could be present. If we accept this and assume that the open form is the reactive one, then its reactivity would be at least 10 times higher than k_{obs}. This would result in an acceleration factor of over 1000 compared to the glycine ester, which is not very convincing, based on the effect of charges as described above. The second possibility (path k_2) represents an external attack of OH^- onto the coordinated ester. The X-ray structure analysis and the spectra in solution could be used to support this mechanism. Compared to the rate of Co^{3+}-promoted hydrolysis of bidentate esters, with an enhancement factor of $\sim 10^6$, however, our value of ~ 100 is modest. This could be due to the relatively weak Cu^{2+} carbonyl interaction (long apical Cu–O bond, *cf. Table 2*), which contrasts with the much stronger Co–O bond. The third possibility, that the hydroxo complex, which is present in small amounts, is the reactive species (path k_3) cannot be excluded. Since in the case of the Cu^{2+}-promoted reaction we do not reach a plateau even at the highest pH studied, we can only give a lower limit for the first-order constant k_3 as $\sim 10^3\ s^{-1}$ (assuming 1% hydroxo complex at pH 13). This value would be extremely high compared to analogous Co^{3+} reactions with rate constants of *ca.* $3 \cdot 10^{-3}\ s^{-1}$ [17]. In conclusion, we can state that path k_1 is very improbable, but for the moment there is no convincing argument to distinguish between an external or an internal OH^- attack in the case of the carboxylates **3–5**.

Finally, a comparison between the reactivity of the different functional groups studied in their Cu^{2+} complexes are such that, at pH 12, the nitrile (**2**) and the carboxylate (**3–5**) groups are hydrolyzed with half times requiring stopped-flow techniques, whereas the phosphonate hydrolysis (**6**) takes hours. The amide **7** does not hydrolyze over a period of 3 days.

The support of this work by the *Swiss National Science Foundation* (Project No. 2000-5.372) is gratefully acknowledged.

REFERENCES

[1] D. Tschudin, A. Basak, Th. A. Kaden, *Helv. Chim. Acta* **1988**, *71*, 100.
[2] see *e.g.* M. N. Hughes, 'The Inorganic Chemistry of Biological Processes', Wiley, New York, 1972.
[3] R. W. Hay, P. J. Morris, *Metal Ions Biol. Syst.* **1976**, *5*, 173.
[4] H. Kroll, *J. Am. Chem. Soc.* **1952**, *74*, 2036.
[5] P. A. Sutton, D. A. Buckingham, *Acc. Chem. Res.* **1987**, *20*, 357.
[6] W. Schibler, Th. A. Kaden, *J. Chem. Soc., Chem. Commun.* **1981**, 603.
[7] D. Tschudin, Th. A. Kaden, *Pure Appl. Chem.* **1988**, *60*, 489.
[8] G. M. Sheldrick, SHELX-76, Program, University of Göttingen.
[9] D. T. Cromer, J. B. Mann, *Acta Crystallogr., Sect. A* **1968**, *24*, 321; D. T. Cromer, D. Libermann, *J. Chem. Phys.* **1970**, *53*, 1891.
[10] H. Gampp, M. Maeder, A. D. Zuberbühler, *Talanta* **1980**, *27*, 1037.
[11] B. Bosnich, C. K. Poon, M. L. Tobe, *Inorg. Chem.* **1965**, *4*, 1102.
[12] J. C. A. Boyens, S. M. Dobson, in 'Stereochemical and Stereophysical Behaviour of Macrocycles', Ed. I. Bernal, Elsevier, Amsterdam, 1987, Vol. 2, p. 1.
[13] R. W. Hay, P. J. Morris, *J. Chem. Soc. (B)* **1970**, 1577.
[14] R. W. Hay, L. J. Porter, *J. Chem. Soc. (B)* **1967**, 1261.
[15] R. W. Hay, K. B. Nolan, *J. Chem. Soc., Dalton Trans.* **1974**, 2542.
[16] D. A. Buckingham, D. M. Forster, A. M. Sargeson, *J. Am. Chem. Soc.* **1969**, *91*, 3451.
[17] E. Baraniak, D. A. Buckingham, C. R. Clark, B. H. Moyniham, A. M. Sargeson, *Inorg. Chem.* **1986**, *25*, 3466.